

DEVELOPMENT OF INDICES OF LARVAL BLUEFIN TUNA (*THUNNUS THYNNUS*) IN THE WESTERN MEDITERRANEAN SEA

G. Walter Ingram, Jr.¹, Francisco Alemany², Diego Alvarez², and Alberto Garcia³

SUMMARY

Fishery independent indices of bluefin tuna larvae in the western Mediterranean Sea are presented utilizing ichthyoplankton survey data collected from 2001 through 2005 by the Spanish Institute of Oceanography. Indices were developed using larval catch rates collected using two different types of bongo gear by employing a delta-lognormal modeling approach, including following covariates: water temperature at 25 m, salinity at 25 m, water depth, time of day, geostrophic water velocities, year, and a gear variable for the combined model.

RÉSUMÉ

Les indices de larves de thon rouge indépendants des pêcheries dans la mer Méditerranée occidentale sont présentés au moyen des données des prospections d'ichthyoplancton recueillies de 2001 à 2005 par l'Institut espagnol d'océanographie. Des indices ont été élaborés au moyen des taux de capture des larves recueillies au moyen de deux types différents d'engin bongo en utilisant une approche de modélisation delta-lognormale, incluant les covariables suivantes : température de l'eau à 25 m, salinité à 25 m, profondeur de l'eau, moment de la journée, vitesses géostrophiques du courant, année, ainsi qu'une variable d'engin pour le modèle combiné.

RESUMEN

Se presentan índices de larvas de atún rojo independientes de la pesquería en el mar Mediterráneo occidental utilizando datos de prospecciones de ictioplancton recopilados desde 2001 hasta 2005 por el Instituto Español de Oceanografía. Los índices se desarrollaron utilizando tasas de captura larval recopiladas utilizando dos tipos diferentes de red bongo y empleando un enfoque delta-lognormal de modelación, que incluía las siguientes covariables: temperatura del agua a 25 m, salinidad a 25 m, profundidad del agua, hora del día, velocidad del agua geostrófica, año y una variable de arte para el modelo combinado.

KEYWORDS

Mathematical models, fish larvae, bluefin tuna

¹ NOAA Fisheries, Southeast Fisheries Science Center, Mississippi Laboratories, 3209 Frederic Street, Pascagoula, MS, 39567, USA, walter.ingram@noaa.gov.

² Instituto Español de Oceanografía, Centro Oceanográfico de Baleares, Muelle de Poniente, s/n, Apdo. 291, 07015 Palma de Mallorca, Baleares, Spain, francisco.alemany@ba.ieo.es, diego.alvarez@ba.ieo.es.

³ Instituto Español de Oceanografía, Centro Oceanográfico de Málaga, Puerto Pesquero, s/n Apdo. 285, 29640 Fuengirola (Málaga), Spain, agarcia@ma.ieo.es.

1. Introduction and Statistical Methodology

Managers became concerned of the status of northern bluefin tuna (*Thunnus thynnus*) stocks in the late 1960's. During recent years, international assessments of Atlantic bluefin tuna (ABT hereafter) have been conducted at least biannually. Most abundance indices used during assessments of Atlantic bluefin tuna were of a fishery dependent nature. Scott *et al.* (1993) presented a spawning biomass index for the western stock, which was based upon the abundance of bluefin tuna larvae collected during fishery independent surveys conducted by NOAA Fisheries in the Gulf of Mexico. Recently, Ingram *et al.* (2010) updated these indices using standardization via delta-lognormal models.

During recent decades ichthyoplankton surveys targeting ABT larvae were conducted in several areas of the Mediterranean Sea, the spawning area of the eastern stock of ABT. However, the surveys employed heterogeneous sampling strategies and methodologies, without any temporal continuity (e.g. Dicenta 1977; Dicenta and Piccinetti 1978; Oray and Karakulak 2005; Piccinetti and Piccinetti-Manfrin 1994; Piccinetti *et al.* 1996a, 1996b, 1997; Tsuji *et al.* 1997). In 2001 the IEO started a series of standardized ichthyoplankton surveys, named TUNIBAL, around the Balearic Islands, recognized as one of the main spawning areas of ABT within the Mediterranean (Garcia *et al.* 2004; Alemany *et al.* 2010), with the aim of characterizing the spawning habitat of this species and deepen in the knowledge of its larval ecology, assessing the influence of environmental factors on larval distribution and abundance. These surveys followed an adaptive sampling strategy, combining intensive sampling of high density larval patches with quantitative sampling over a systematic grid of stations. The ABT larval abundance data gathered during these surveys are useful for developing an index of abundance, which would represent the second fishery-independent index of abundance of ABT in the world, and currently the only fishery-independent index concerning the eastern Atlantic stock. Therefore, the objective of this report is to present abundance indices of ABT larvae collected around the Balearic Islands based on delta-lognormal models.

The data considered for achieving this objective come from the surveys carried out from 2001 to 2005. In each of those years around 200 stations, located over the nodes of a regular grid of 10 x 10 nautical miles, covering most of the known ABT spawning areas in this region (from 37.85° to 40.35° N and from 0.77° to 4.91° E), were sampled during the spawning peak of the species in the Western Mediterranean. The exact number of sampled stations and the dates of the surveys are shown in **Table 1**.

The sampling methodologies are described in detail in Alemany *et al.* (2010). ABT larvae were collected by oblique tows performed down to 70 meters in the open sea or down to 5 m above the sea floor in shallower stations, using a 333 µm mesh fitted to 60 cm mouth opening Bongo nets. In addition, subsurface tows between 3 m deep and surface were carried out at the same stations in 2004 and 2005 by means of a Bongo 90 net equipped with a 500 µm mesh. In both type of hauls, flowmeters were fitted to the net mouths for determination of the volume of water filtered. Plankton samples were fixed on board with 4% formaldehyde in seawater. In the laboratory, all fish larvae were sorted under a stereoscopic microscope. Tuna larvae were then identified to species level. In addition, at each station, a vertical profile of temperature, salinity, oxygen, turbidity, fluorescence and pressure was obtained using a CTD probe SBE911. The vertical profiles extended to the 300-dbar level, although a selected set of profiles extended up to 650 dbar to establish a reference for geopotential topographies. The temperature, salinity and pressure were then used to obtain the geopotential field with reference to 600-dbar, a level that has historically been demonstrated and used as the non-motion level in the Balearic Sea. Geostrophic velocities were then calculated in relation to this non-motion level.

The delta-lognormal index of relative abundance (I_y) as described by Lo *et al.* (1992) was estimated as

$$(1) \quad I_y = c_y p_y,$$

where c_y is the estimate of mean CPUE for positive catches only for year y ; p_y is the estimate of mean probability of occurrence during year y . Both c_y and p_y were estimated using generalized linear models. Data used to estimate abundance for positive catches (c) and probability of occurrence (p) were assumed to have a lognormal distribution and a binomial distribution, respectively, and modeled using the following equations:

$$(2) \quad \ln(\mathbf{c}) = \mathbf{X}\boldsymbol{\beta} + \boldsymbol{\varepsilon}$$

and

$$(3) \quad \mathbf{p} = \frac{e^{\mathbf{X}\boldsymbol{\beta} + \boldsymbol{\varepsilon}}}{1 + e^{\mathbf{X}\boldsymbol{\beta} + \boldsymbol{\varepsilon}}}, \text{ respectively,}$$

where \mathbf{c} is a vector of the positive catch data, \mathbf{p} is a vector of the presence/absence data, \mathbf{X} is the design matrix for main effects, $\boldsymbol{\beta}$ is the parameter vector for main effects, and $\boldsymbol{\varepsilon}$ is a vector of independent normally distributed errors with expectation zero and variance σ^2 .

We used the GLIMMIX and MIXED procedures in SAS (v. 9.1, 2004) to develop the binomial and lognormal submodels, respectively. Similar covariates were tested for inclusion for both submodels to develop separate indices for the bongo-60 and bongo-90: water temperature at 25 m, salinity at 25 m, water depth (m), time of day (two categories: night, if solar altitude was negative; day, if solar altitude was positive), geostrophic velocities from processing CTD data (cm/sec), and year. A variable for gear-type (bongo-60 or bongo-90) was included for testing in each submodel when developing the index for both bongo-60 or bongo-90 data combined. A backward selection procedure was used to determine which variables were to be included into each submodel based on type 3 analyses with a level of significance for inclusion of $\alpha = 0.05$. If year was not significant then it was forced into each submodel in order to estimate least-squares means for each year, which are predicted annual population margins (i.e., they estimate the marginal annual means as if over a balanced population). The fit of each of the submodels were evaluated using AIC and residual analyses.

Therefore, c_y and p_y were estimated as least-squares means for each year along with their corresponding standard errors, $SE(c_y)$ and $SE(p_y)$, respectively. From these estimates, I_y was calculated, as in equation (1), and its variance calculated as

$$(4) \quad V(I_y) \approx V(c_y)p_y^2 + c_y^2V(p_y) + 2c_y p_y \text{Cov}(c, p),$$

where

$$(5) \quad \text{Cov}(c, p) \approx \rho_{c,p} [SE(c_y)SE(p_y)],$$

and $\rho_{c,p}$ denotes correlation of c and p among years.

2. Results and Discussion

Table 2 summarizes the data used in these analyses. Sampling occurred during June and July, and the number of stations per year ranged from 173 to 205 for the bongo-60 gear and from 197 to 217 for the bongo-90 gear. Sizes of larvae collected in the bongo-60 gear ranged from 1.39 to 8.5 mm. Length data for the bongo-90 gear is currently unavailable.

The backward selection procedure used to develop the delta-lognormal model for the bongo-60 data is summarized in **Table 3**. For the binomial submodel, all variables except year and salinity were dropped. The AIC for model run #5 increased as geostrophic velocity was dropped from the model indicating a possible increase in lack-of-fit. However, due to the large p -value (0.3554) of the type 3 test for the inclusion of geostrophic velocity in model run #4, we chose to remove this variable. For the lognormal submodel, all variables were dropped from the model except year, which had a high p -value (0.4997) of the type 3 test for inclusion (**Table 3**). **Figure 1** summarizes the resulting indices, and Figures 2 and 3 contain diagnostic plots for model development. Due to the binomial nature of the presence absence data modeled with the binomial submodel, the residuals plotted in **Figure 2** have bimodal tendencies. Another way to evaluate binomial model performance was by using AUC [Area Under Curve; the curve being a ROC (Receiver Operating Curve)] methodology presented by Steventon *et al.* (2005). The AUC value for the binomial submodel for the bongo-60 data was 0.6378. This means that in 64 out of 100 instances, a station selected at random from those with larvae had a higher predicted probability of larvae being present than a station randomly selected from those that had no larvae. The residual plots in Figure 3 indicate the approximately normal distribution of the residuals of the lognormal submodel.

The backward selection procedure used to develop the delta-lognormal model for the bongo-90 data is summarized in Table 4. For the binomial submodel, all variables except year and salinity were dropped, and the AIC for each model run decreased as the insignificant variables was dropped from the model indicating an increase in parsimony. For the lognormal submodel, all variables were dropped from the model except year and

water depth (**Table 4**). The AIC for model runs #4 and #5 increased as salinity and temperature were dropped from the model, respectively, indicating a possible increase in lack-of-fit. However, due to the large p -values of the type 3 test for inclusion of these variables at the time they were dropped (0.2482 and 0.1316, respectively), we chose to remove these variables. Figure 4 summarizes the resulting indices, and **Figures 5 and 6** contain diagnostic plots for model development. Again, the binomial submodel residuals plotted in **Figure 5** have bimodal tendencies. The AUC value for the binomial submodel for the bongo-90 data was 0.6659. This means that in 67 out of 100 instances, a station selected at random from those with larvae had a higher predicted probability of larvae being present than a station randomly selected from those that had no larvae. The residual plots in Figure 6 indicate the approximately normal distribution of the residuals of the lognormal submodel.

The backward selection procedure used to develop the delta-lognormal model for both the bongo-60 and bongo-90 data combined is summarized in **Table 5**. For the binomial submodel, all variables except year, gear-type and salinity were dropped. The AIC for model run #5 increased as geostrophic velocity was dropped from the model indicating a possible increase in lack-of-fit. However, due to the insignificant p -value (0.0762) of the type 3 test for the inclusion of geostrophic velocity in model run #4, we chose to remove this variable. For the lognormal submodel, all variables were dropped from the model except year and gear-type (**Table 5**). The AIC for each of the model runs increased as variables were dropped from the model, except for model run #6, indicating a possible increase in lack-of-fit. However, due to the large p -values of the type 3 test for inclusion of these variables at the time they were dropped, we chose to remove these variables. **Figure 7** summarizes the resulting indices, and **Figures 8 and 9** contain diagnostic plots for model development. Again, the binomial submodel residuals plotted in Figure 8 have bimodal tendencies. The AUC value for the binomial submodel for the bongo-90 data was 0.6609. This means that in 66 out of 100 instances, a station selected at random from those with larvae had a higher predicted probability of larvae being present than a station randomly selected from those that had no larvae. The residual plots in Figure 9 indicate the approximately normal distribution of the residuals of the lognormal submodel.

3. References

- Alemany, F., L. Quintanilla, P. Velez-Belchí, A. García, D. Cortés, J.M. Rodríguez, M.L. Fernández de Puelles, C. González-Pola and J.L. López-Jurado. 2010. Characterization of the spawning habitat of Atlantic bluefin tuna and related species in the Balearic Sea (western Mediterranean). *Progress in Oceanography*. 86 (1-2): 21-38. CLimate Impacts on Oceanic TOP Predators (CLIOTOP) – International Symposium.
- Dicenta, A. 1977. Zonas de puesta del atún (*Thunnus thynnus*) y otros túnidos del Mediterráneo occidental y primer intento de evaluación del “stock” de reproductores de atún. *Boletín del Instituto Español de Oceanografía*. 234: 109-135.
- Dicenta, A. and C. Piccinetti. 1978. Desove de atún (*Thunnus thynnus* L.) en el Mediterráneo Occidental y evaluación directa del stock de reproductores basado en la abundancia de sus larvas. *Collective Volumes of Scientific Papers of ICCAT*. 7(2): 389-395.
- García, A., Alemany F., Velez-Belchí P., López Jurado J.L., Cortés D., de la Serna J.M., González Pola C., Rodríguez J.M., Jansá J. and T. Ramírez. 2004. Characterization of the bluefin tuna spawning habitat off the Balearic archipelago in relation to key hydrographic features and associated environmental conditions. CGPM/ICCAT 7th Joint Ad-hoc meeting, May, Málaga, 2004.
- Ingram, G. W., Jr., W. J. Richards, J. T. Lamkin and B. Muhling. 2010. Annual indices of Atlantic bluefin tuna (*Thunnus thynnus*) larvae in the Gulf of Mexico developed using delta-lognormal and multivariate models. *Aquatic Living Resources*. 23: 35-47.
- Lo, N. C. H., L.D. Jacobson, and J.L. Squire. 1992. Indices of relative abundance from fish spotter data based on delta-lognormal models. *Can. J. Fish. Aquat. Sci.* 49: 2515-1526.
- Oray, I. K. and F.F. Karakulak. 2005. Further evidence of spawning of bluefin tuna (*Thunnus thynnus* L., 1758) and the tuna species (*Auxis rochei* L., 1810, *Euthynnus alletteratus* Raf., 1810) in the eastern Mediterranean Sea: preliminary results of TUNALEV larval survey in 2004. *Journal of Applied Ichthyology*. 21: 226-240.

- Piccinetti, C. and G. Piccinetti Manfrin. 1994. Distribution des larves de Thonidés en Méditerranée. FAO fisheries Report. 494: 186, 206.
- Piccinetti, C., Piccinetti-Manfrin G. and S. Soro. 1996a. Larve di tunnidi in Mediterraneo. *Biologia Marina Mediterranea*. 3(1): 303-309.
- Piccinetti, C., Piccinetti-Manfrin G., and S. Soro. 1996b. Résultats d'une campagne de recherche sur les larves de thonidés en Méditerranée. SCRS, 57.
- Piccinetti, C., Piccinetti-Manfrin G. and S. Soro. 1997. Résultats d'une campagne de recherche sur les larves de thonidés en Méditerranée. ICCAT. Collective Volume of Scientific Papers. 46: 207-214.
- Scott, G. P., S.C. Turner, C.B. Grimes, W.J. Richards, and E.B. Brothers. 1993. Indices of larval bluefin tuna, *Thunnus thynnus*, abundance in the Gulf of Mexico; modeling variability in growth, mortality, and gear selectivity. *Bull. Mar. Sci.* 53(2):912-929.
- Steventon, J.D., W.A. Bergerud and P.K. Ott. 2005. Analysis of presence/absence data when absence is uncertain (false zeroes): an example for the northern flying squirrel using SAS[®]. Res. Br., B.C. Min. For. Range, Victoria, B.C. Exten. Note 74.
- Tsuji, S., Segawa K. and Y. Hiroe. 1997. Distribution and abundance of *Thunnus* larvae and their relation to the oceanographic condition in the Gulf of Mexico and the Mediterranean Sea during May through August of 1994. Collective Volumes of Scientific Papers of ICCAT. 46(2): 161-176.

Table 1. Surveys realized within the framework of TUNIBAL project.

<i>Survey</i>	<i>Year</i>	<i>R/V</i>	<i>Dates</i>	<i>Number of stations</i>
TUNIBAL 0601	2001	Vizconde de Eza	15 June–10 July	185
TUNIBAL 0602	2002	Vizconde de Eza	5 June–30 June	203
TUNIBAL 0703	2003	Cornide de Saavedra	4 July–30 July	199
TUNIBAL 0604	2004	Cornide de Saavedra	18 June–10 July	194
TUNIBAL 0605	2005	Cornide de Saavedra	27 June–23 July	221

Table 2. Summary of data used in these analyses. B60 and B90 gear type indicate bongo-60 and bongo-90 gear, respectively.

<i>Gear</i>	<i>Survey Year</i>	<i>Number of Stations Used in Analysis</i>	<i>Start Date</i>	<i>End Date</i>	<i>Number of Specimens</i>	<i>Mean Length (mm)</i>	<i>Size Range (mm)</i>
B60	2001	173	17-Jun-01	7-Jul-01	123	3.634	2.0 - 7.0
B60	2002	205	7-Jun-02	29-Jun-02	332	2.820	2.0 - 6.0
B60	2003	199	3-Jul-03	29-Jul-03	211	2.709	2.0 - 8.0
B60	2004	181	22-Jun-04	10-Jul-04	265	3.760	2.0 - 8.5
B60	2005	204	28-Jun-05	23-Jul-05	182	3.046	1.39 - 8.0
B90	2004	197	22-Jun-04	9-Jul-04	3300	NA	NA
B90	2005	217	28-Jun-05	23-Jul-05	866	NA	NA

Table 3. Backward selection procedure for building delta-lognormal submodels for the bongo-60 data.

<i>Model Run #1</i>	<i>Binomial Submodel Type 3 Tests (AIC 4473.7)</i>						<i>Lognormal Submodel Type 3 Tests (AIC 446.0)</i>			
	<i>Num DF</i>	<i>Den DF</i>	<i>Chi-Square</i>	<i>F Value</i>	<i>Pr > ChiSq</i>	<i>Pr > F</i>	<i>Num DF</i>	<i>Den DF</i>	<i>F Value</i>	<i>Pr > F</i>
<i>Year</i>	4	882	11.91	2.98	0.0180	0.0186	4	120	0.51	0.7270
<i>Day/Night</i>	1	882	0.36	0.36	0.5494	0.5495	1	120	0.37	0.5443
<i>Water Depth</i>	1	882	0.19	0.19	0.6644	0.6645	1	120	0.01	0.9327
<i>Temperature at 25 m</i>	1	882	0.21	0.21	0.6487	0.6488	1	120	0.86	0.3549
<i>Salinity at 25m</i>	1	882	9.71	9.71	0.0018	0.0019	1	120	0.28	0.6008
<i>Geostrophic Velocity</i>	1	882	0.92	0.92	0.3365	0.3368	1	120	0.07	0.7890

<i>Model Run #2</i>	<i>Binomial Submodel Type 3 Tests (AIC 4460.3)</i>						<i>Lognormal Submodel Type 3 Tests (AIC 430.3)</i>			
	<i>Num DF</i>	<i>Den DF</i>	<i>Chi-Square</i>	<i>F Value</i>	<i>Pr > ChiSq</i>	<i>Pr > F</i>	<i>Num DF</i>	<i>Den DF</i>	<i>F Value</i>	<i>Pr > F</i>
<i>Year</i>	4	883	11.91	2.98	0.0180	0.0185	4	121	0.54	0.7049
<i>Day/Night</i>	1	883	0.40	0.40	0.5255	0.5257	1	121	0.36	0.5475
<i>Water Depth</i>	dropped						dropped			
<i>Temperature at 25 m</i>	1	883	0.12	0.12	0.7326	0.7327	1	121	0.95	0.3313
<i>Salinity at 25m</i>	1	883	12.16	12.16	0.0005	0.0005	1	121	0.31	0.5757
<i>Geostrophic Velocity</i>	1	883	0.89	0.89	0.3450	0.3453	1	121	0.07	0.7975

<i>Model Run #3</i>	<i>Binomial Submodel Type 3 Tests (AIC 4454.4)</i>						<i>Lognormal Submodel Type 3 Tests (AIC 431.7)</i>			
	<i>Num DF</i>	<i>Den DF</i>	<i>Chi-Square</i>	<i>F Value</i>	<i>Pr > ChiSq</i>	<i>Pr > F</i>	<i>Num DF</i>	<i>Den DF</i>	<i>F Value</i>	<i>Pr > F</i>
<i>Year</i>	4	884	12.26	3.06	0.0156	0.0160	4	124	0.68	0.6095
<i>Day/Night</i>	1	884	0.41	0.41	0.5234	0.5236	1	124	0.25	0.6191
<i>Water Depth</i>	dropped						dropped			
<i>Temperature at 25 m</i>	dropped						1	124	0.83	0.3649
<i>Salinity at 25m</i>	1	884	13.08	13.08	0.0003	0.0003	1	124	0.38	0.5398
<i>Geostrophic Velocity</i>	1	884	0.87	0.87	0.3502	0.3504	dropped			

<i>Model Run #4</i>	<i>Binomial Submodel Type 3 Tests (AIC 4451.3)</i>						<i>Lognormal Submodel Type 3 Tests (AIC 430.6)</i>			
	<i>Num DF</i>	<i>Den DF</i>	<i>Chi-Square</i>	<i>F Value</i>	<i>Pr > ChiSq</i>	<i>Pr > F</i>	<i>Num DF</i>	<i>Den DF</i>	<i>F Value</i>	<i>Pr > F</i>
<i>Year</i>	4	885	12.21	3.05	0.0159	0.0164	4	125	0.71	0.5897
<i>Day/Night</i>	dropped						dropped			
<i>Water Depth</i>	dropped						dropped			
<i>Temperature at 25 m</i>	dropped						1	125	0.81	0.3691
<i>Salinity at 25m</i>	1	885	12.85	12.85	0.0003	0.0004	1	125	0.41	0.5222
<i>Geostrophic Velocity</i>	1	885	0.85	0.85	0.3552	0.3554	dropped			

Model Run #5	<i>Binomial Submodel Type 3 Tests (AIC 4475.7)</i>						<i>Lognormal Submodel Type 3 Tests (AIC 430.9)</i>			
<i>Effect</i>	<i>Num DF</i>	<i>Den DF</i>	<i>Chi-Square</i>	<i>F Value</i>	<i>Pr > ChiSq</i>	<i>Pr > F</i>	<i>Num DF</i>	<i>Den DF</i>	<i>F Value</i>	<i>Pr > F</i>
<i>Year</i>	4	894	12.00	3.00	0.0173	0.0178	4	126	0.65	0.6284
<i>Day/Night</i>	dropped						dropped			
<i>Water Depth</i>	dropped						dropped			
<i>Temperature at 25 m</i>	dropped						1	126	1.35	0.2471
<i>Salinity at 25m</i>	1	894	15.21	15.21	<.0001	0.0001	dropped			
<i>Geostrophic Velocity</i>	dropped						dropped			
Model Run #6	<i>Binomial Submodel Type 3 Tests (AIC 4475.7)</i>						<i>Lognormal Submodel Type 3 Tests (AIC 460.2)</i>			
<i>Effect</i>	<i>Num DF</i>	<i>Den DF</i>	<i>Chi-Square</i>	<i>F Value</i>	<i>Pr > ChiSq</i>	<i>Pr > F</i>	<i>Num DF</i>	<i>Den DF</i>	<i>F Value</i>	<i>Pr > F</i>
<i>Year</i>	4	894	12.00	3.00	0.0173	0.0178	4	138	0.84	0.4997
<i>Day/Night</i>	dropped						dropped			
<i>Water Depth</i>	dropped						dropped			
<i>Temperature at 25 m</i>	dropped						dropped			
<i>Salinity at 25m</i>	1	894	15.21	15.21	<.0001	0.0001	dropped			
<i>Geostrophic Velocity</i>	dropped						dropped			

Table 4. Backward selection procedure for building delta-lognormal submodels for the bongo-90 data.

Model Run #1	<i>Binomial Submodel Type 3 Tests (AIC 1822.2)</i>						<i>Lognormal Submodel Type 3 Tests (AIC 364.5)</i>			
<i>Effect</i>	<i>Num DF</i>	<i>Den DF</i>	<i>Chi-Square</i>	<i>F Value</i>	<i>Pr > ChiSq</i>	<i>Pr > F</i>	<i>Num DF</i>	<i>Den DF</i>	<i>F Value</i>	<i>Pr > F</i>
<i>Year</i>	1	380	7.38	7.38	0.0066	0.0069	1	87	1.07	0.3040
<i>Day/Night</i>	1	380	1.91	1.91	0.1674	0.1682	1	87	0.58	0.4497
<i>Water Depth</i>	1	380	2.89	2.89	0.0889	0.0897	1	87	2.71	0.1031
<i>Salinity at 25m</i>	1	380	6.39	6.39	0.0115	0.0119	1	87	1.34	0.2511
<i>Temperature at 25 m</i>	1	380	1.71	1.71	0.1910	0.1918	1	87	3.94	0.0503
<i>Geostrophic Velocity</i>	1	380	4.14	4.14	0.0418	0.0425	1	87	0.82	0.3688
Model Run #2	<i>Binomial Submodel Type 3 Tests (AIC 1815.6)</i>						<i>Lognormal Submodel Type 3 Tests (AIC 364.6)</i>			
<i>Effect</i>	<i>Num DF</i>	<i>Den DF</i>	<i>Chi-Square</i>	<i>F Value</i>	<i>Pr > ChiSq</i>	<i>Pr > F</i>	<i>Num DF</i>	<i>Den DF</i>	<i>F Value</i>	<i>Pr > F</i>
<i>Year</i>	1	381	6.42	6.42	0.0113	0.0117	1	88	1.07	0.3039
<i>Day/Night</i>	1	381	2.15	2.15	0.1428	0.1436	dropped			
<i>Water Depth</i>	1	381	1.62	1.62	0.2034	0.2042	1	88	3.00	0.0866
<i>Salinity at 25m</i>	1	381	11.93	11.93	0.0006	0.0006	1	88	1.91	0.1707
<i>Temperature at 25 m</i>	dropped						1	88	4.40	0.0387
<i>Geostrophic Velocity</i>	1	381	3.91	3.91	0.0479	0.0486	1	88	0.92	0.3389

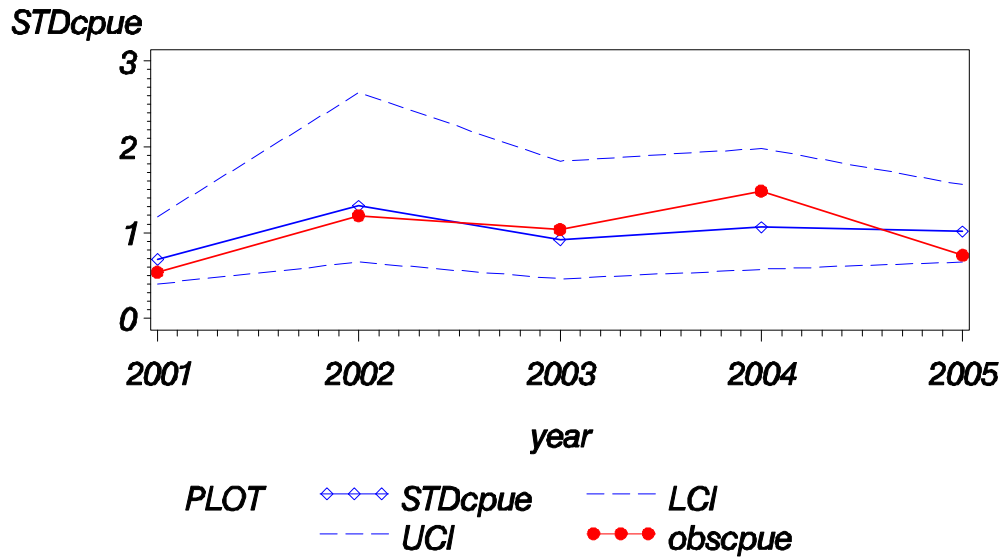
Model Run #3		<i>Binomial Submodel Type 3 Tests (AIC 1802.4)</i>					<i>Lognormal Submodel Type 3 Tests (AIC 360.6)</i>			
<i>Effect</i>	<i>Num DF</i>	<i>Den DF</i>	<i>Chi-Square</i>	<i>F Value</i>	<i>Pr > ChiSq</i>	<i>Pr > F</i>	<i>Num DF</i>	<i>Den DF</i>	<i>F Value</i>	<i>Pr > F</i>
<i>Year</i>	1	382	6.66	6.66	0.0099	0.0102	1	89	0.88	0.3502
<i>Day/Night</i>	1	382	2.38	2.38	0.1227	0.1236	dropped			
<i>Water Depth</i>	dropped						1	89	3.76	0.0557
<i>Salinity at 25m</i>	1	382	15.65	15.65	<.0001	<.0001	1	89	1.35	0.2482
<i>Temperature at 25 m</i>	dropped						1	89	3.58	0.0618
<i>Geostrophic Velocity</i>	1	382	3.51	3.51	0.0611	0.0618	dropped			
Model Run #4		<i>Binomial Submodel Type 3 Tests (AIC 1795.2)</i>					<i>Lognormal Submodel Type 3 Tests (AIC 362.7)</i>			
<i>Effect</i>	<i>Num DF</i>	<i>Den DF</i>	<i>Chi-Square</i>	<i>F Value</i>	<i>Pr > ChiSq</i>	<i>Pr > F</i>	<i>Num DF</i>	<i>Den DF</i>	<i>F Value</i>	<i>Pr > F</i>
<i>Year</i>	1	383	6.56	6.56	0.0104	0.0108	1	90	0.54	0.4654
<i>Day/Night</i>	dropped						dropped			
<i>Water Depth</i>	dropped						1	90	4.85	0.0301
<i>Salinity at 25m</i>	1	383	14.46	14.46	0.0001	0.0002	dropped			
<i>Temperature at 25 m</i>	dropped						1	90	2.32	0.1316
<i>Geostrophic Velocity</i>	1	383	3.43	3.43	0.0641	0.0649	dropped			
Model Run #5		<i>Binomial Submodel Type 3 Tests (AIC 1781.7)</i>					<i>Lognormal Submodel Type 3 Tests (AIC 421.3)</i>			
<i>Effect</i>	<i>Num DF</i>	<i>Den DF</i>	<i>Chi-Square</i>	<i>F Value</i>	<i>Pr > ChiSq</i>	<i>Pr > F</i>	<i>Num DF</i>	<i>Den DF</i>	<i>F Value</i>	<i>Pr > F</i>
<i>Year</i>	1	384	7.26	7.26	0.0071	0.0074	1	108	0.89	0.3465
<i>Day/Night</i>	dropped						dropped			
<i>Water Depth</i>	dropped						1	108	8.76	0.0038
<i>Salinity at 25m</i>	1	384	16.01	16.01	<.0001	<.0001	dropped			
<i>Temperature at 25 m</i>	dropped						dropped			
<i>Geostrophic Velocity</i>	dropped						dropped			

Table 5. Backward selection procedure for building delta-lognormal submodels for the bongo-60 and bongo-90 data combined.

Model Run #1		<i>Binomial Submodel Type 3 Tests (AIC 6281.3)</i>					<i>Lognormal Submodel Type 3 Tests (AIC 804.3)</i>			
<i>Effect</i>	<i>Num DF</i>	<i>Den DF</i>	<i>Chi-Square</i>	<i>F Value</i>	<i>Pr > ChiSq</i>	<i>Pr > F</i>	<i>Num DF</i>	<i>Den DF</i>	<i>F Value</i>	<i>Pr > F</i>
<i>Year</i>	4	1268	19.94	4.98	0.0005	0.0005	4	213	0.78	0.5380
<i>Gear</i>	1	1268	6.74	6.74	0.0094	0.0095	1	213	4.11	0.0440
<i>Day/Night</i>	1	1268	1.67	1.67	0.1961	0.1964	1	213	1.97	0.1617
<i>Water Depth</i>	1	1268	1.91	1.91	0.1667	0.1669	1	213	1.54	0.2161
<i>Temperature at 25 m</i>	1	1268	1.56	1.56	0.2115	0.2117	1	213	1.32	0.2524
<i>Salinity at 25m</i>	1	1268	16.03	16.03	<.0001	<.0001	1	213	0.42	0.5161
<i>Geostrophic Velocity</i>	1	1268	3.60	3.60	0.0578	0.0580	1	213	0.00	0.9980

odel Run #2		<i>Binomial Submodel Type 3 Tests (AIC 6271.9)</i>					<i>Lognormal Submodel Type 3 Tests (AIC 805.7)</i>			
<i>Effect</i>	<i>Num DF</i>	<i>Den DF</i>	<i>Chi-Square</i>	<i>F Value</i>	<i>Pr > ChiS q</i>	<i>Pr > F</i>	<i>Num DF</i>	<i>Den DF</i>	<i>F Value</i>	<i>Pr > F</i>
<i>Year</i>	4	1269	19.02	4.75	0.0008	0.0008	4	216	0.96	0.4295
<i>Gear</i>	1	1269	6.75	6.75	0.0094	0.0095	1	216	4.15	0.0428
<i>Day/Night</i>	1	1269	1.81	1.81	0.1786	0.1789	1	216	1.73	0.1903
<i>Water Depth</i>	1	1269	1.02	1.02	0.3119	0.3121	1	216	1.24	0.2662
<i>Temperature at 25 m</i>	dropped						1	216	1.72	0.1907
<i>Salinity at 25m</i>	1	1269	22.20	22.20	<.0001	<.0001	1	216	0.57	0.4518
<i>Geostrophic Velocity</i>	1	1269	3.38	3.38	0.0659	0.0661	dropped			
Model Run #3		<i>Binomial Submodel Type 3 Tests (AIC 6262.0)</i>					<i>Lognormal Submodel Type 3 Tests (AIC 806.0)</i>			
<i>Effect</i>	<i>Num DF</i>	<i>Den DF</i>	<i>Chi-Square</i>	<i>F Value</i>	<i>Pr > ChiS q</i>	<i>Pr > F</i>	<i>Num DF</i>	<i>Den DF</i>	<i>F Value</i>	<i>Pr > F</i>
<i>Year</i>	4	1270	19.67	4.92	0.0006	0.0006	4	217	0.86	0.4917
<i>Gear</i>	1	1270	6.70	6.70	0.0097	0.0098	1	217	4.33	0.0387
<i>Day/Night</i>	1	1270	2.02	2.02	0.1557	0.1560	1	217	1.96	0.1628
<i>Water Depth</i>	dropped						1	217	1.71	0.1924
<i>Temperature at 25 m</i>	dropped						1	217	1.23	0.2686
<i>Salinity at 25m</i>	1	1270	27.38	27.38	<.0001	<.0001	dropped			
<i>Geostrophic Velocity</i>	1	1270	3.22	3.22	0.0727	0.0730	dropped			
Model Run #4		<i>Binomial Submodel Type 3 Tests (AIC 6251.1)</i>					<i>Lognormal Submodel Type 3 Tests (AIC 891.8)</i>			
<i>Effect</i>	<i>Num DF</i>	<i>Den DF</i>	<i>Chi-Square</i>	<i>F Value</i>	<i>Pr > ChiS q</i>	<i>Pr > F</i>	<i>Num DF</i>	<i>Den DF</i>	<i>F Value</i>	<i>Pr > F</i>
<i>Year</i>	4	1271	19.47	4.87	0.0006	0.0007	4	246	1.14	0.3395
<i>Gear</i>	1	1271	6.70	6.70	0.0097	0.0098	1	246	6.77	0.0098
<i>Day/Night</i>	dropped						1	246	2.19	0.1402
<i>Water Depth</i>	dropped						1	246	2.28	0.1322
<i>Temperature at 25 m</i>	dropped						dropped			
<i>Salinity at 25m</i>	1	1271	26.34	26.34	<.0001	<.0001	dropped			
<i>Geostrophic Velocity</i>	1	1271	3.15	3.15	0.0760	0.0762	dropped			
Model Run #5		<i>Binomial Submodel Type 3 Tests (AIC 6263.9)</i>					<i>Lognormal Submodel Type 3 Tests (AIC 892.2)</i>			
<i>Effect</i>	<i>Num DF</i>	<i>Den DF</i>	<i>Chi-Square</i>	<i>F Value</i>	<i>Pr > ChiS q</i>	<i>Pr > F</i>	<i>Num DF</i>	<i>Den DF</i>	<i>F Value</i>	<i>Pr > F</i>
<i>Year</i>	4	1280	19.35	4.84	0.0007	0.0007	4	247	1.26	0.2857
<i>Gear</i>	1	1280	6.72	6.72	0.0095	0.0097	1	247	6.40	0.0120
<i>Day/Night</i>	dropped						dropped			
<i>Water Depth</i>	dropped						1	247	2.56	0.1110
<i>Temperature at 25 m</i>	dropped						dropped			
<i>Salinity at 25m</i>	1	1280	30.64	30.64	<.0001	<.0001	dropped			
<i>Geostrophic Velocity</i>	dropped						dropped			

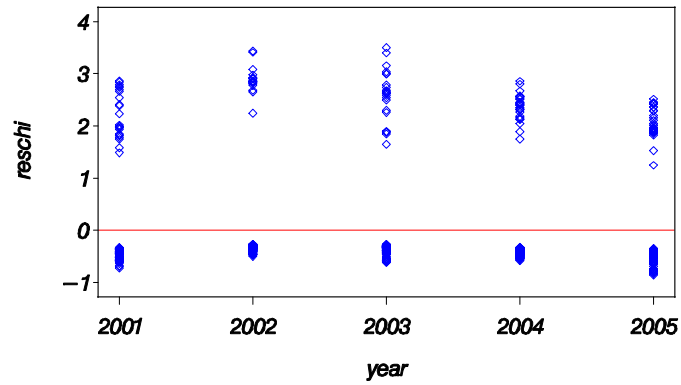
Model Run #6	<i>Binomial Submodel Type 3 Tests (AIC 6263.9)</i>					<i>Lognormal Submodel Type 3 Tests (AIC 878.1)</i>				
	<i>Effect</i>	<i>Num DF</i>	<i>Den DF</i>	<i>Chi-Square</i>	<i>F Value</i>	<i>Pr > ChiSq</i>	<i>Pr > F</i>	<i>Num DF</i>	<i>Den DF</i>	<i>F Value</i>
<i>Year</i>	4	1280	19.35	4.84	0.0007	0.0007	4	248	0.89	0.4734
<i>Gear</i>	1	1280	6.72	6.72	0.0095	0.0097	1	248	7.23	0.0077
<i>Day/Night</i>	dropped					dropped				
<i>Water Depth</i>	dropped					dropped				
<i>Temperature at 25 m</i>	dropped					dropped				
<i>Salinity at 25m</i>	1	1280	30.64	30.64	<.0001	<.0001	dropped			
<i>Geostrophic Velocity</i>	dropped					dropped				



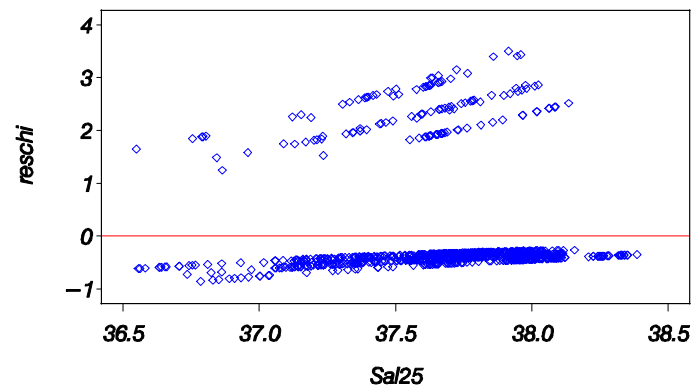
Survey Year	Frequency	N	Index	Scaled Nominal	Scaled Index	CV	LCL	UCL
2001	0.16185	173	0.32946	0.54048	0.69097	0.27449	0.40304	1.18458
2002	0.12683	205	0.62566	1.19887	1.31219	0.35877	0.65426	2.63172
2003	0.12121	198	0.43832	1.03799	0.91930	0.35589	0.46079	1.83405
2004	0.14917	181	0.50728	1.48562	1.06392	0.31839	0.57149	1.98066
2005	0.18627	204	0.48330	0.73704	1.01362	0.21744	0.65946	1.55798

Figure 1. Abundance indices for larval Atlantic bluefin tuna collected with the bongo-60 gear in the western Mediterranean Sea. STDcpue is the index scaled to a mean of one over the time series. Obscpue is the average nominal CPUE, and LCI and UCI are 95% confidence limits. In the table below, the *frequency* listed is nominal frequency, *N* is the number of bottom longline stations, *Index* is the abundance index in CPUE units, *Scaled Index* is the index scaled to a mean of one over the time series, *CV* is the coefficient of variation on the index value, and *LCL* and *UCL* are 95% confidence limits.

a. Chi-square residuals by year.



b. Chi-square residuals by salinity at 25 m.



c. QQplot of chi-square residuals.

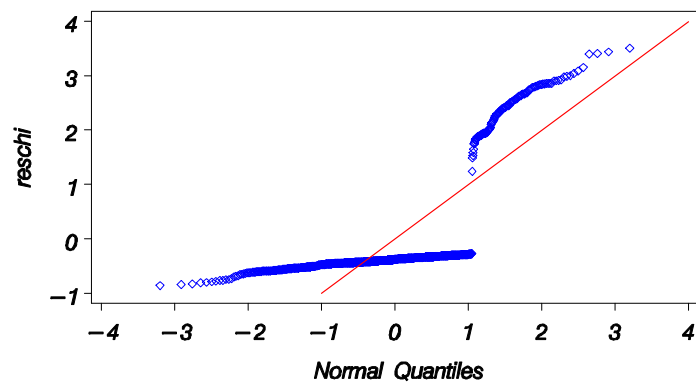
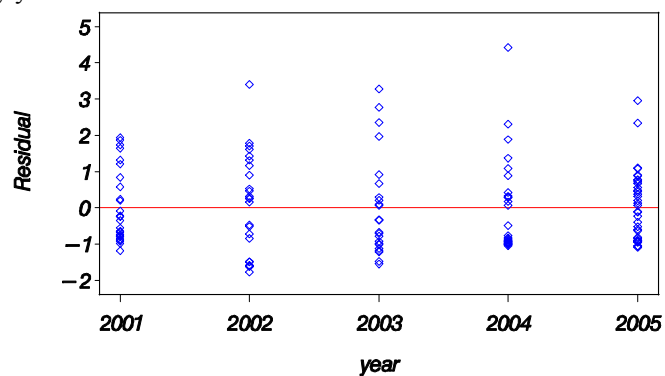


Figure 2. Diagnostic residual plots of the binomial submodel for larval Atlantic bluefin tuna collected with the bongo-60 gear in the western Mediterranean Sea.

a. Chi-square residuals by year.



b. QQplot of chi-square residuals.

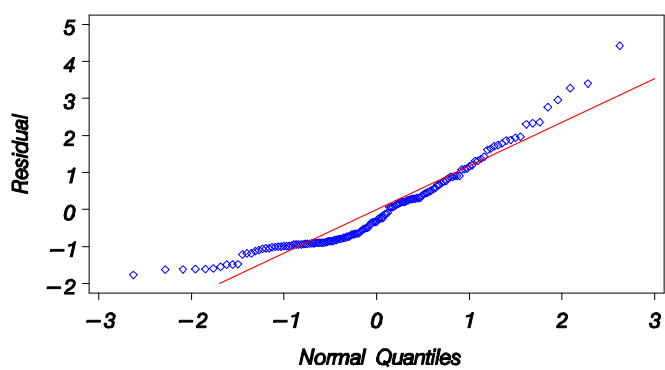
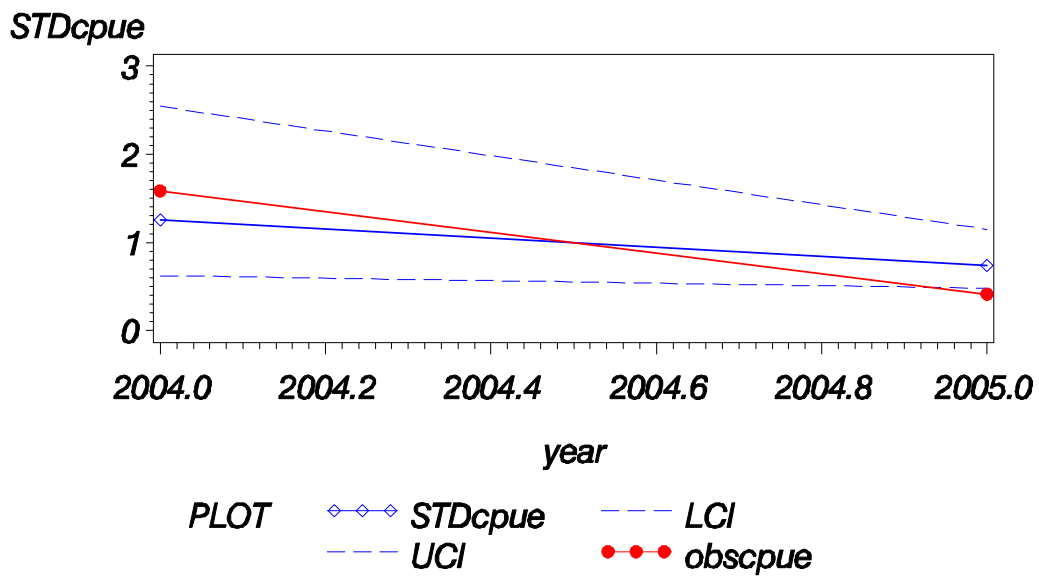


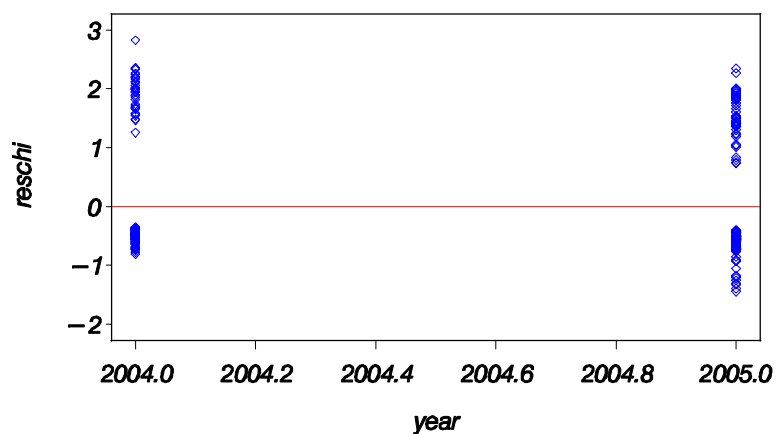
Figure 3. Diagnostic residual plots of the lognormal submodel for larval Atlantic bluefin tuna collected with the bongo-60 gear in the western Mediterranean Sea.



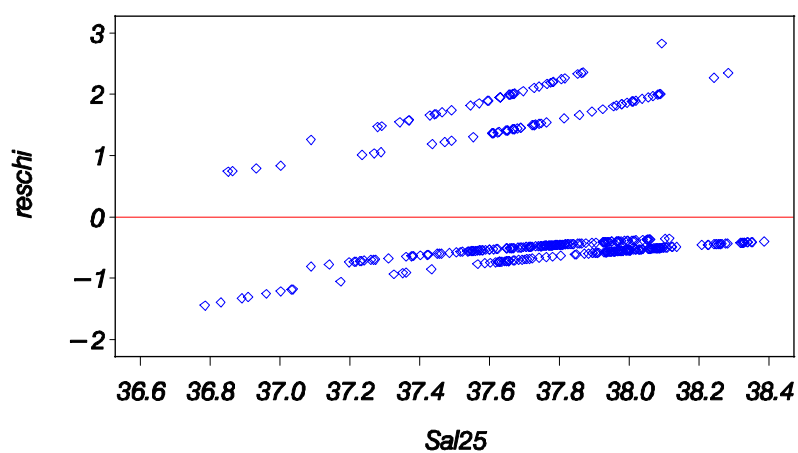
<i>Survey Year</i>	<i>Frequency</i>	<i>N</i>	<i>Index</i>	<i>Scaled Nominal</i>	<i>Scaled Index</i>	<i>CV</i>	<i>LCL</i>	<i>UCL</i>
2004	0.22335	197	0.84901	1.58573	1.25851	0.36298	0.62271	2.54349
2005	0.30876	217	0.50022	0.41427	0.74149	0.22091	0.47919	1.14737

Figure 4. Abundance indices for larval Atlantic bluefin tuna collected with the bongo-90 gear in the western Mediterranean Sea. STDcpue is the index scaled to a mean of one over the time series. Obscpue is the average nominal CPUE, and LCI and UCI are 95% confidence limits. In the table below, the *frequency* listed is nominal frequency, *N* is the number of bottom longline stations, *Index* is the abundance index in CPUE units, *Scaled Index* is the index scaled to a mean of one over the time series, *CV* is the coefficient of variation on the index value, and *LCL* and *UCL* are 95% confidence limits.

a. Chi-square residuals by year.



b. Chi-square residuals by salinity at 25 m.



c. QQplot of chi-square residuals.

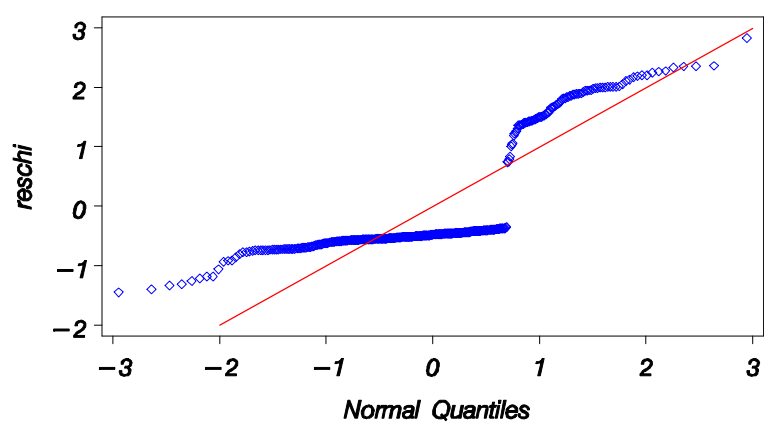
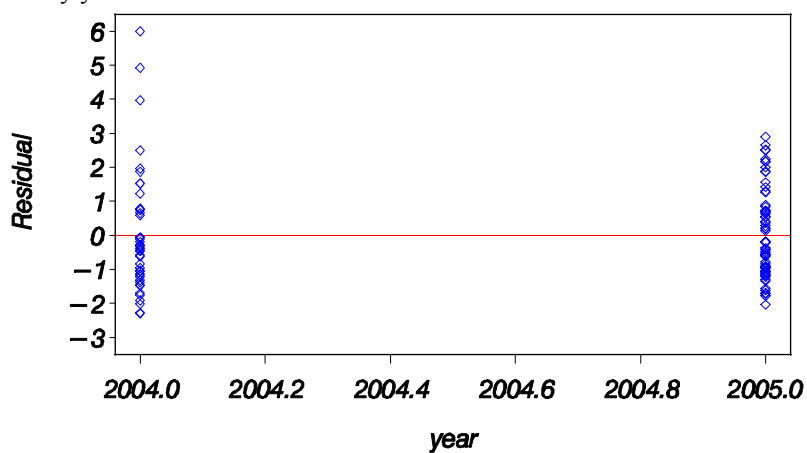
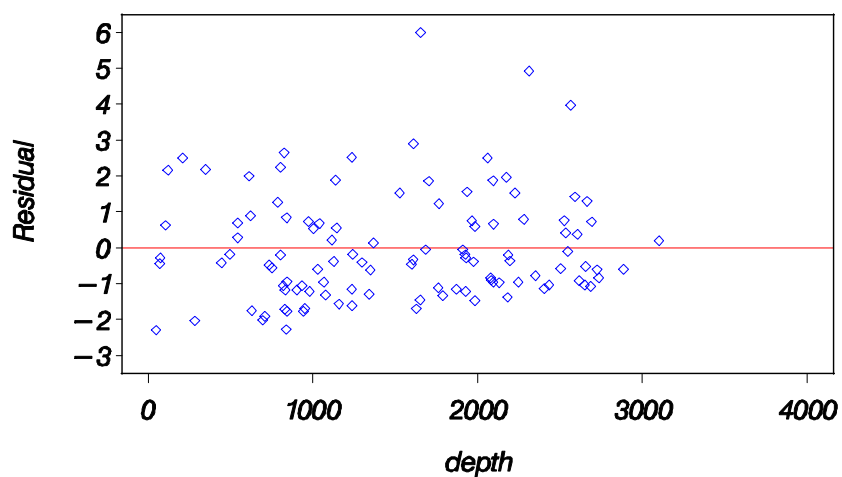


Figure 5. Diagnostic residual plots of the binomial submodel for larval Atlantic bluefin tuna collected with the bongo-90 gear in the western Mediterranean Sea.

a. Chi-square residuals by year.



b. Chi-square residuals by water depth.



c. QQplot of chi-square residuals.

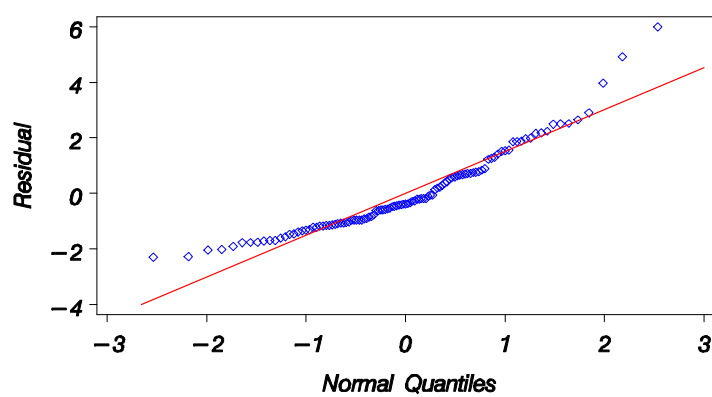
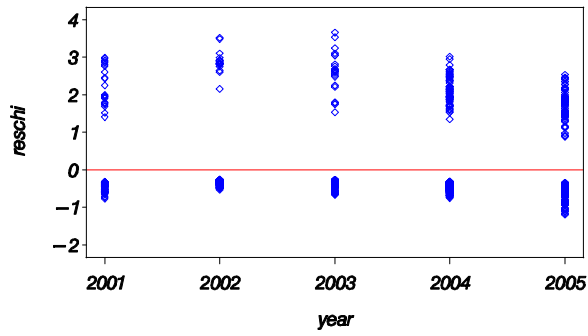
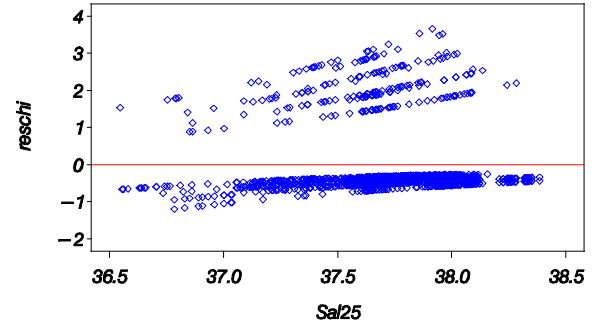


Figure 6. Diagnostic residual plots of the lognormal submodel for larval Atlantic bluefin tuna collected with the bongo-90 gear in the western Mediterranean Sea.

a. Chi-square residuals by year.



c. Chi-square residuals by salinity at 25 m.



b. Chi-square residuals by gear-type.



d. QQplot of chi-square residuals.

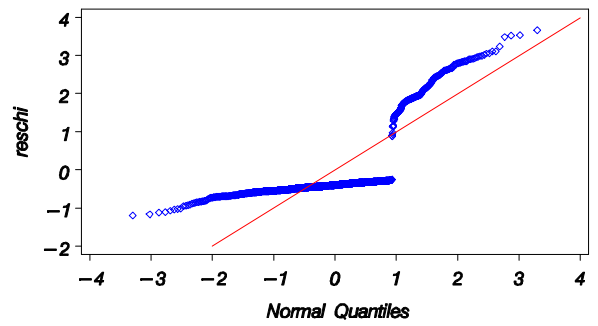
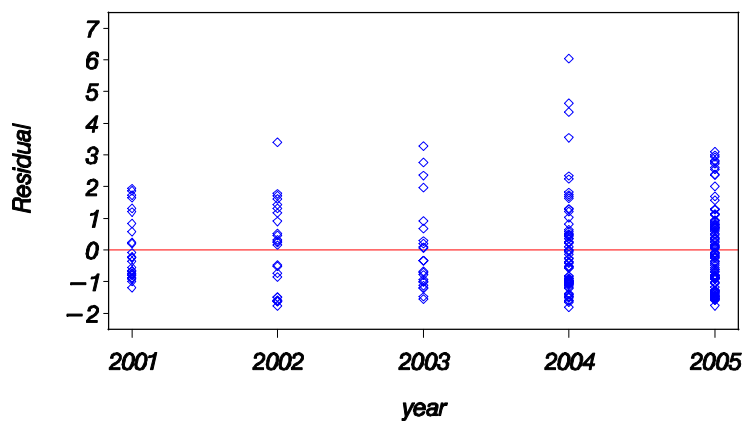
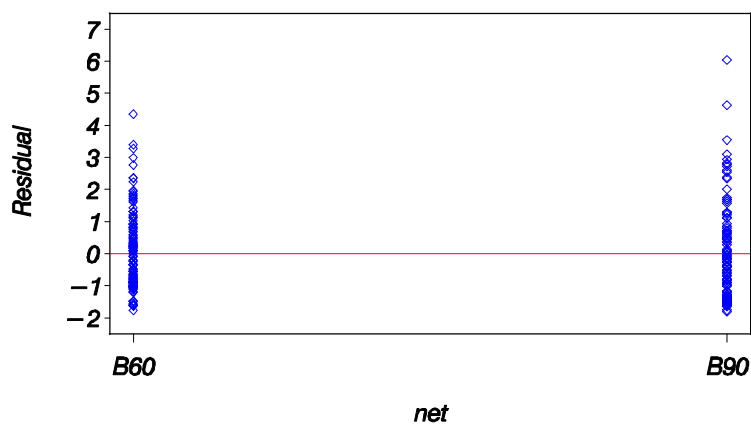


Figure 8. Diagnostic residual plots of the binomial submodel for larval Atlantic bluefin tuna collected with both the bongo-60 and bongo-90 gear in the western Mediterranean Sea.

a. Chi-square residuals by year.



b. Chi-square residuals by gear-type.



c. QQplot of chi-square residuals.

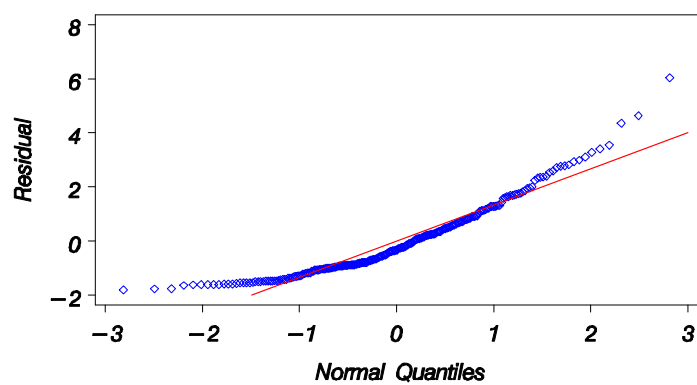


Figure 9. Diagnostic residual plots of the lognormal submodel for larval Atlantic bluefin tuna collected with both the bongo-60 and bongo-90 gear in the western Mediterranean Sea.